Materials Reliability Program (MRP)
Crack Growth Rates for Evaluating Primary Water Stress Corrosion Cracking (PWSCC) of Thick-Wall Alloy 600 Material (MRP-55)

Non-proprietary version

July 18, 2002

Prepared by:
PWR Materials Reliability Program Alloy 600 Issues Task Group

Materials Reliability Program (MRP)
Crack Growth Rates for Evaluating Primary Water Stress Corrosion Cracking (PWSCC) of Thick-Wall Alloy 600 Material (MRP-55)

Summary

The Materials Reliability Program (MRP) has developed a recommended crack growth rate (CGR) curve for primary water stress corrosion cracking (PWSCC) of thick-wall components fabricated from Alloy 600 material such as reactor vessel head (RVH) nozzles including CRDM, CEDM, and In-Core Instrument (ICI) nozzles. The recommended curve is not applicable to Alloy 600 steam generator tubes, which are thin-walled. The CGR curve is based on controlled testing of fracture mechanics specimens fabricated using 22 heats of CRDM nozzle, thick-wall tube, rolled bar, and forged bar material and 4 heats of plate material. Specifically, tests conducted at Westinghouse in the U.S., Studsvik in Sweden, EDF and CEA in France, and CIEMAT in Spain were considered in the evaluation presented here. Such testing allows careful control of applied load (stress intensity factor) and temperature and also allows accurate measurement of CGR. In accordance with standard practice for evaluation of SCC, a power-law dependence on stress intensity factor was assumed. This was based upon the well-established relationship originally developed by Scott [1,2] from examination of PWSCC in steam generator tube materials, since insufficient test data were available for any one heat of thick-wall Alloy 600 material over an appropriately wide range of stress intensity factors.

Evaluation of the laboratory data on a heat-by-heat basis resulted in a log-normal distribution of CGR curves that describes the observed variability in crack growth rates. The MRP recommended CGR curve corresponds to the 75th percentile level of this distribution. As such, the recommended curve may be interpreted as the mean of the upper half of the distribution describing the variability in CGR due to material heat. The MRP recommended curve can be applied directly to disposition detected PWSCC flaws such as axial flaws in RVH nozzle base metal material.

However, the MRP recommends that a multiplicative factor increasing the CGR be considered for evaluating the growth of hypothetical circumferential flaws connected to the OD of RVH nozzles above the elevation of the J-groove weld. Because of current uncertainties in the exact composition of the chemical environment in contact with the nozzle OD, the MRP recommends that a factor of 2 increase in CGR be conservatively applied for deterministic evaluations of the growth of such hypothetical above-weld defects. Evaluation of the growth of such circumferential flaws is required in deterministic risk assessments of potential RVH nozzle ejection and any consequential increase in core damage frequency. However, it is expected that any actual circumferential flaws detected above the J-groove weld would be repaired before plant startup.

This report documents the development of the MRP CGR curve for Alloy 600 base metal including example calculations of the time for axial and circumferential PWSCC cracks in RVH nozzles to grow to a larger size. It begins with a detailed examination of the environment expected on the OD of the RVH nozzle above the J-groove weld if a leak path forms due to axial cracking through the base metal and/or cracking of the J-groove attachment weld. This work shows that there is unlikely to be a significant increase in the growth rate of cracks in contact with the OD chemical environment compared to the growth rate of cracks in the normal primary water environment.

Specifically, the likely environments responsible for SCC of Alloy 600 in the annulus between a penetration and the reactor upper head are either (1) normal PWR primary water, (2) hydrogenated, superheated steam, or—generally less likely—(3) concentrated PWR water. The hydrogenated, superheated steam environment is expected to result in crack growth rates close in magnitude to those for normal primary water. In addition, because the most likely high-temperature pH_T for the concentrated PWR water environment is close to the range for normal primary water, the third possible environment is also expected to result in crack growth rates close in magnitude to those for normal primary water.

The EPRI-MRP CGR review team, an international panel of experts in the area of SCC crack growth, provided input to the MRP in the evaluation of the OD environment and the development of the recommended CGR curve. This group met to review the available worldwide data on August 10, 2001, in Lake Tahoe, Nevada, on October 2–4, 2001, in Airlie, Virginia [3], and on March 6–8, 2002, in Dallas, Texas, and held additional periodic discussions.[*] MRP activities in the area of PWSCC growth rates are ongoing in 2002.

Introduction

Recent incidents of stress corrosion cracking of Alloy 600 components other than steam generator tubes in the primary circuits of PWRs have highlighted the need for a qualified equation for crack growth rates to evaluate flaws found by in-service inspection. A similar requirement has also been identified for Alloy 182/82 weldments following observations of cracking in primary circuit welds with high residual stresses and in some J-groove welds attaching CRDM nozzles to the reactor upper head. The crack growth behavior of the weld metals will be the subject of a separate report in 2002, and the remainder of this document applies only to Alloy 600 base material.

Previously, a crack growth equation based on primary water induced cracking of roll transitions of steam generator tubes—typically known as the modified Scott equation—has been used to predict crack growth of other Alloy 600 primary circuit components [1,2]. The fact that it was based on non-destructive examination data from a large number of susceptible heats appears to have ensured over a ten-year period that it has remained a useful point of reference for other product forms, and it plays an important role in the present analysis. Few heats of material for

[*] Note that not all sections of this report reflect the views of each member of the CGR review team. E.g., EDF advocated a different and earlier approach to the development of CGR curves than that presented here. The EDF approach is consistent with the regulatory structure in France, which differs from the regulatory structure in the U.S.

upper head penetrations tested to date have shown growth rates exceeding those predicted by the equation developed from the steam generator tube data [1,2]. Nevertheless, the databases for other product forms (e.g. CRDM head penetration material) of Alloy 600 have increased to the point where more direct evaluations of crack growth behavior can be attempted.

An additional issue concerns cases where cracking has appeared to initiate on the external surface of Alloy 600 CRDM nozzles just above the J-groove weld following a leak of primary water into the annulus between the nozzle and the upper head. This cracking has been observed to extend circumferentially following the root of the J-groove weld. In this case, it is necessary to consider the phase state and chemical composition of the fluid as leaking primary water boils, flashes to steam, and depressurizes to atmospheric pressure in the containment at a high temperature maintained by the steel mass of the upper head.

To summarize, qualified crack growth rate equations are required for the following conditions:

- Alloy 600 nozzle material in PWR primary water,
- Alloy 600 in the environment(s) created by primary water exiting along a leak path.

These topics were addressed by an EPRI-MRP CGR review team comprising an international panel of experts in the area of SCC crack growth [3]. The results of their deliberations formed a key input to this report. An assessment of the likely limits to the above described leak scenario is discussed first, followed by an assessment of the crack growth database of laboratory tests performed in normal specification PWR primary water and, finally, application of the results to disposition of axial flaws—and evaluation of hypothetical circumferential flaws—in RVH nozzles.

Possible Environments Responsible for External Surface Cracking of RVH Nozzles

Evaluation of external cracking in Alloy 600 CRDM nozzles just above the J-groove weld is confronted with potential uncertainty as to the nature of the environment in a leak path as PWR primary water boils and flashes to steam at the temperature of the upper head. Nevertheless, the review group agreed that several bounding conditions could be defined as discussed below. In addition, the question of possible back diffusion of air into the annulus environment and the possible influence of impurities from the original fabrication or from the containment atmosphere are addressed.

Oxygen availability/consumption

It was agreed by the review group that back diffusion of oxygen into the crevice environment could be disregarded [3]. Two independent assessments based on molecular diffusion models of oxygen from air against a counter flow of escaping steam were examined (see Appendices B2 and B4 in [3]). They showed that oxygen cannot penetrate to the end of the crevice between the nozzle and the upper head with radial clearances between 13 to 38 μm (0.5 to 1.5 mils) except at very low mass flow rates of steam. Such leak rate conditions would be nearly stagnant at an order of magnitude below that which has been typically observed in the field (4 kg in an 18 month operating cycle or 4×10^{-4} kg/hr (8×10^{-4} lb/hr or 2×10^{-6} gpm) as evidenced by small

quantities of boric acid crystal deposits at the locations where the nozzles penetrate the holes in the vessel head [4]).

It should be noted that chemical reaction between oxygen and the metal walls of the crevice was not included in the above calculations. It is well known in aqueous corrosion science that crevices typically 25 to 100 μm (1 to 4 mils) wide (and much narrower cracks) are always de-oxygenated due to rapid consumption of any incoming oxygen by general corrosion on the crevice walls very near the mouth.

A third factor militating against the presence of oxygen in the annulus between the CRDM nozzles and the upper head is the presence of hydrogen, both in the leaking primary water and diffusing through the upper head. This will maintain a relatively reducing crevice environment, as discussed in more detail below.

In conclusion, oxygenated crevice environments are highly unlikely for the relatively long and narrow crevice geometry of the annulus between the CRDM nozzle and upper head penetration.

Phase state considerations

In order to establish the limits within which the environment created from boiling PWR primary water can evolve, it is necessary to consider first how the physical state, liquid or vapor phase, may change. The upper head temperature in U.S. plants can be between 286 and 318°C (547 to 605°F) dependent on plant design [5]. Two separate studies were considered by the review group [3]. For radial clearances between the CRDM nozzle and upper head of 13 to 38 μm (0.5 to 1.5 mils) and leak rates from 4×10^{-5} to 4×10^{-3} kg/hr (8×10^{-5} to 8×10^{-3} lb/hr or 2×10^{-7} to 2×10^{-5} gpm), the pressure drop in the annulus was less than 1 atm and steam velocities ranged from 1 to 100 cm/s (0.4 to 40 in/s). Thus in this case, primary water flashes to steam within the leaking stress corrosion crack crossing the CRDM penetration or the J-groove weld. On the other hand, for a leak rate of 0.04 kg/hr (0.08 lb/hr or 2×10^{-4} gpm) and a specification interference fit of 90 μm (3.5 mils) as fabricated, the boiling transition was calculated to occur very high in the annulus, the pressure drop across the leaking crack being negligible by comparison in this case.

Thus, it can be concluded that the variability in dimensions of the interference fits between penetrations and upper heads coupled with the presence of very tight stress corrosion cracks in a penetration or J-weld means that the boiling transition can occur virtually anywhere along the leak path. Therefore, the environment immediately above the J-weld during a leak event can be:

- superheated steam if the pressure drop to the saturated vapor pressure occurs within the stress corrosion crack, or
- boiling and consequently concentrated PWR primary water if boiling occurs at the exit of the stress corrosion crack, or
- normal PWR primary water when the boiling transition is well above the J-weld.

The second step is to consider the chemical limits for each of the above mentioned phase states. The behavior of the three main components in boiling primary water—hydrogen, lithium hydroxide, and boric acid—must be considered.

Crevice chemistry—hydrogen

The review group came to the following consensus on the behavior of hydrogen in a crevice between a CRDM nozzle and an upper head penetration and its key role in determining stress corrosion susceptibility of Alloy 600 in addition to the applied stress and temperature [3].

Hydrogen diffuses readily through steel at temperatures of ~300°C (~572°F) from PWR primary water to the outside of the pressure vessel. Thus for practical purposes, even if hydrogen is partitioned preferentially to the vapor phase at a boiling transition, the diffusion kinetics of hydrogen through the surrounding metal are such that a dynamic equilibrium will be maintained with the hydrogen in the metal at temperature. This effective hydrogen partial pressure will depend on the diffusion profile through the upper head thickness but it can be assumed to be equal to or less than that of normal PWR primary water.

Thus, two of the most likely environments in the crevice above the J-weld for initiating and propagating stress corrosion cracks in Alloy 600 must be either hydrogenated, superheated steam or normal PWR water. The effective hydrogen concentration in both environments is sufficient to maintain the corrosion potential close to that of the Ni/NiO equilibrium, which is the key chemical parameter determining the stress corrosion susceptibility of nickel based alloys. Consequently, stress corrosion susceptibility of Alloy 600 is similar in both phases at the same temperature. It is also noted that even if the concentration of hydrogen was depleted by local boiling, electrochemical coupling between low alloy steel and Alloy 600 would lower the corrosion potential of Alloy 600 into the same range as that controlled by the normal hydrogen partial pressure of PWR primary water. This would ensure a similar susceptibility to stress corrosion cracking as in normal specification PWR primary water.

Crevice chemistry—lithium hydroxide and boric acid

It was deduced earlier that the boiling transition along the leak path of primary water could occur virtually anywhere from within a crack in the wall of the CRDM nozzle or its J-weld to high in the annulus well above the J-groove weld. Thus, it is argued that for the boiling transition to be situated just near to the top of the J-weld would be an unlikely event. Nevertheless, in such a case it is necessary to consider the liquid phase compositions that may be created by boiling concentration of lithium hydroxide and boric acid in PWR primary water. Three independent studies to define such liquid phase environments were examined by the review group [3]. All relied on calculations using the EPRI code MULTEQ, with or without models incorporating limits imposed by the mass flow kinetics through the annulus between the CRDM nozzle and upper head. These calculations assumed that the mass flow rates were low enough such that the temperature did not drop significantly, which implies that the leak rate is well below 1 liter/h (0.004 gpm).[*] Despite different input assumptions, the three studies came to very similar conclusions as summarized below.

[*] While 1 liter/h (0.004 gpm) produced a large change in temperature in a CEA experiment, calculations for a more realistic geometry in connection with the French unit Bugey 3 predict little change in temperature for this leak rate (see Appendix B1 in [3]).

As PWR primary water flashes to steam, lithium hydroxide and boric acid can concentrate near the liquid/vapor interface. Despite the volatility of boric acid relative to lithium hydroxide, MULTEQ calculations at constant temperature (313°C (595°F)) and mass flow rate suggest that these components will concentrate until lithium metaborate, $LiBO_2$, precipitates. At this point, lithium hydroxide is concentrated sufficiently to give a high-temperature pH_T estimated at 8 to 8.6, dependent on input assumptions, with a boiling point elevation of less than 3°C (5°F). Towards the end of a fuel cycle when boric acid is much less concentrated in primary water, the pH_T due to boiling is predicted to reach 9.4. These calculated values of pH_T are significantly higher than 6.8 to 7.4 of normal PWR primary water but are not particularly "caustic." The low boiling point elevation suggests that very little liquid is present. Nevertheless, such a solution buffered at a pH_T of 8 to 9.4 is one conceivable liquid phase environment at the boiling transition, albeit with a hydrogen overpressure equal to or less than that of normal PWR primary water as discussed earlier.

It should be noted that lithium metaborate incorporated into the above calculations exhibits retrograde solubility with increasing temperature above 47°C (117°F), so slightly more alkaline pH_T values could be expected at lower boiling temperatures.

An alternative model has considered very low leak rates so that boiling occurs very rapidly with no mixing with any remaining liquid within the annulus. In this case, MULTEQ with lithium metaborate again as the precipitating species predicts that the environment evolves initially in the alkaline direction to a maximum pH_T of about 8 and then in the acidic direction to pH_T values of 4 to 6 (for various primary water compositions at 313°C (595°F)). The pH_T shift in the acid direction is limited by B_2O_3 precipitation. (Note that pure water at the same temperature has a pH_T of 5.8.) Thus an alternative concentrated environment is dominated by boric acid, again at the approximate hydrogen overpressure of PWR primary water.

A weakness of the MULTEQ calculations so far summarized is that the chemical and electrochemical reactions with the metal components of the annulus are not included. The practical situation involves a small volume of water and a very large surface area of Alloy 600 on one side of the crevice and low alloy steel on the other. Practical laboratory experience shows that boric acid solutions at ~300°C (~572°F) react fairly rapidly with low alloy steel to produce insoluble borates, and the pH_T is consequently buffered at near neutral values by iron hydroxide in solution, provided the amounts of boric acid are low (as assumed in the calculations). A modified MULTEQ calculation incorporating iron metaborate as a possible solid precipitate in boiling PWR primary water has shown that, for low rates of leakage into the annulus, its very low solubility should ensure that the pH_T does not shift significantly in the acid direction.

Further clues to the chemical nature of the environment in a boiling crevice are provided by studies of deposits on PWR fuel pins that are responsible for the "Axial Offset Anomaly." Analyses suggest that boron is precipitated not as lithium metaborate but as nickel boroferrite, Ni_2FeBO_5, otherwise known as the mineral bonaccordite. This precipitate forms on fuel pins even at the low concentrations of iron normally present in PWR primary water. Nickel boroferrite is very likely to be much less soluble in water than lithium metaborate, or even iron metaborate, and to incorporate lithium readily into its crystal structure, but it does not yet appear

in the thermodynamic database of MULTEQ. Such a low solubility would severely limit the possible movement of pH relative to normal PWR primary water. Thus, it is concluded that if iron is not incorporated into MULTEQ calculations, the degree to which concentration and change of pH can take place—before precipitation intervenes to limit it—can be seriously overestimated.

Two final pieces of information available to the review group relating to environments created from boiling PWR primary water concerned two French experiments simulating such a leak. The first test simulated a leak at a rate of 1 liter/h (0.004 gpm) (see Appendix B1 in [3]). Along with a mass of boric acid crystals formed at the leak site, several complex borates were detected such as $Li_2B_4O_7$, $FeB_4O_7(8H_20)$, and $Li_3B_5O_8(OH)_2$ from which the pH_T of the liquid phase was estimated to be between 7 and 8. A complication in the interpretation of this experiment was an initial fall in temperature at the beginning of the leak, which could have affected the type of precipitates formed. Nevertheless, this experiment demonstrates the potential complexity of borate precipitates and that their nature is such as to restrict significantly the movement of pH of the liquid phase when PWR primary water boils. The second test [6] allowed the composition of a fixed volume of slowly concentrating primary water (1500 ppm B and 2.1 ppm Li) to be determined as a function of concentration factor. Introducing the experimentally determined composition into the MULTEQ software produced a pH_T in the range of 4.3 to 4.7 for the experimental temperature of 300°C (572°F).

To summarize, in the specific case of the boiling transition zone, the environment is most likely to have a composition and high-temperature pH_T close to those of normal PWR primary water even if extreme values between 4 and 9.4 can be calculated using the existing thermodynamic database of MULTEQ. Specifically, the pH_T is expected to have a maximum value of 7.5 to 8, except perhaps for a limited time period near the end of the fuel cycle. The effective partial pressure of hydrogen, as described earlier, is assumed to be similar to that of PWR primary water, with any changes in hydrogen partial pressure not expected to significantly affect crack growth rates. The situation described above would not exist, however, if the leak rates were sufficiently high to result in a large, local decrease in temperature and appreciable corrosion of low-alloy steel.

Influence of other impurities

Normal quality assurance cleaning practices during assembly of the CRDM nozzles in upper heads should guarantee a high degree of cleanliness of the annulus between the nozzle and the upper head penetration.* Deposition of atmospheric aerosols containing mainly sulfates and chlorides as the main pollutants of concern would be the only significant source of pollutants afterwards.

Flow of steam through the annulus between a CRDM nozzle and an upper head penetration following a leak through a crack in the nozzle or its J-groove weld would tend to clean any residual impurities such as chloride and sulfate from the annulus since these impurities are sparingly soluble in pure superheated steam. This flow would tend to reduce their influence

* *Original footnote considered proprietary..*

because, unlike the chemicals added deliberately to PWR water, their supply to the annulus is limited.

If the presence of such impurities must be assumed, the influence of chloride can at least be judged from data in the literature [8]. Alloys with greater than 40% nickel have excellent resistance to stress corrosion in standard test environments such as boiling magnesium chloride. They are not totally immune, however, in concentrated boric acid solutions contaminated with chloride at 100 to 360°C (212 to 680°F). When the concentration of chloride was very high (2 to 50 g/l) in the absence of oxygen or at low ppm concentrations in the presence of oxygen, transgranular or intergranular stress corrosion was observed. Sensitization was also an aggravating factor. The presence of oxygen has already been discounted in the CRDM nozzle crevice environment, and very high concentrations of chloride are not credible. Thus the potential for this type of chloride induced stress corrosion cracking appears negligible.

Sulfate contamination is potentially more significant for nickel based alloys such as Alloy 600 than chloride contamination. Sulfate is known to be the main active species causing intergranular stress corrosion cracking (IGSCC) of Alloy 600 in the so-called "doped" steam test where 30 ppm each of sulfate, chloride, fluoride, and sometimes nitrate as their sodium salts are added to hydrogenated, superheated steam, typically at 400°C (752°F). Stress corrosion lives of Alloy 600 are reduced by an order of magnitude relative to pure hydrogenated steam. Unpublished Framatome data show that the adverse effect of the impurities persists at impurity concentrations reduced by one order of magnitude from those in the classic, doped steam test, but not when reduced by two orders of magnitude (i.e. to around 0.3 ppm). Given both the measures taken to ensure cleanliness during fabrication and the flushing effect in the OD annulus once a leak from the primary side develops, possible levels of contamination are expected to be well below this. Thus no significant effect of such pollutants would be anticipated.

Summary of relevant metal/environment combinations

Three material/environment combinations are considered pertinent to current concerns with Alloy 600 and nickel base weld metals of PWR upper head penetrations:

- Alloys 600 and 182/82 in normal PWR primary water,
- Alloy 600 in concentrated PWR water but with at a high-temperature pH_T close to that of normal primary water, and
- Alloy 600 in hydrogenated, superheated steam.

Of these, that with concentrated PWR primary water is considered least likely to be practically relevant since it is based on the requirement that the boiling zone be situated at the maximum residual stress zone just above the J-weld.

The situation described above would not exist, however, if the leak rates were sufficiently high to result in a large, local decrease in temperature and appreciable corrosion of low-alloy steel.

Influence of pH

It is generally accepted that the influence of pH within the PWR primary water specification on stress corrosion susceptibility is small with a possible slight enhancement at the higher end of the normal range of 7.4. One study is available of crack growth rates between pH_T values of 5 and 8.5 at a temperature of 330°C (626°F) and at a pH_T of 9 at 350°C (662°F) [9,10]. It shows no significant effect of pH on crack growth rates between pH_T values of 5 and 7.5. However, for solutions of higher pH, there is an observed increase in CGR proportional to the second power of pH_T for stress intensity factors in the range of 30 to 60 MPa$\sqrt{m}$ (27 to 55 ksi$\sqrt{in}$):

$$CGR \propto \left(\frac{pH_T}{7.5} \right)^2 \quad \text{for } 7.5 \le pH_T \le 9 \qquad [1]$$

Given that the maximum expected pH_T during most of the fuel cycle is about 8, the expected increase in CGR due to the slightly elevated pH environment is on the order of 15%.* Conservatively assuming a pH_T of 9 in the crevice environment would result in an acceleration factor of around 1.5.

Conclusions

The most likely environments responsible for stress corrosion cracking of Alloy 600 in the annulus between a penetration and the upper head are either hydrogenated, superheated steam or normal PWR primary water. Based on laboratory tests in high-temperature, hydrogenated steam environments [11,12,13,14], the CGRs in the possible hydrogenated, superheated steam environment will be similar to those in normal PWR primary water at the same temperature.

Oxygen from air cannot penetrate significantly into the crevice between the CRDM nozzle and the upper head penetration and is not relevant to the practical problem.

If the boiling interface happens to be close to the topside of the J-weld, itself a low probability occurrence, concentration of PWR primary water solutes, lithium hydroxide and boric acid, can in principle occur. However, as will be clear below, the potential effect of the slightly elevated pH due to the concentrated PWR environment is rather small compared to the scatter observed in the database of laboratory CGR data evaluated by the MRP. As previously mentioned, the analysis presented here assumes that leak rates are low enough to ensure that a large, local decrease in temperature and appreciable corrosion of low-alloy steel do not occur. Plant experience has shown that this is the usual case [4].

Therefore, the MRP recommends that the CGRs for laboratory tests performed in normal primary water be used as the basis for evaluation of the growth of SCC flaws exposed to the annular crevice environment between RVH nozzles and the reactor upper head. However, given the current uncertainties in the exact composition of the chemical environment on the RVH nozzle OD, including the potential effect of a slightly elevated pH, the MRP also suggests that a

* The typical primary water environment used in the tests that produced the data compiled in this report is 1000–1200 ppm boron and 2.0–2.2 ppm lithium at 325°C, resulting in a pH_T of 7.3.

multiplicative factor of 2 be considered when applying the results of these CGR tests to evaluate the growth of such OD flaws.

Development of a CGR Curve for Alloy 600 RVH Nozzle Base Metal

Power-law relationship

There is general agreement that crack growth in Alloy 600 materials in the primary water environment can be modeled using a stress intensity factor relationship with differences in temperature accounted for by an activation energy (Arrhenius) model for thermally controlled processes:

$$\dot{a} = \exp\left[-\frac{Q_g}{R}\left(\frac{1}{T}-\frac{1}{T_{ref}}\right)\right]\alpha\left(K-K_{th}\right)^{\beta} \qquad [2]$$

where:

$\dot{a}$	=	crack growth rate at temperature T
Q_g	=	thermal activation energy for crack growth
R	=	universal gas constant
T	=	absolute operating temperature at location of crack
T_{ref}	=	absolute reference temperature used to normalize data
α	=	crack growth amplitude
K	=	crack tip stress intensity factor
K_{th}	=	crack tip stress intensity factor threshold
β	=	exponent

Establishment of CGR database

The final database of CGRs compiled in accordance with the deliberations of the CGR review team includes 158 data points from tests performed by Westinghouse [1], Studsvik [15], EDF [16,17,18], CEA [16,19,20], and CIEMAT [21,22,23,24,25] covering the full temperature range tested (290°C (554°F) to 363°C (686°F)). The laboratories concerned confirmed that their test procedures took account of the key technical issues identified by the review team for assessing data quality when quantifying CGRs (see Table 1) [3]. Note, however, that independent checks by the review team were not carried out on all specimens. The resulting CGR database used to develop the MRP CGR curve is shown in Table 2. For completeness, Appendix A to this report contains those laboratory CGR data points that were originally assembled by the MRP team but then excluded from the development of the MRP CGR curve. Appendix A indicates the main reason why each of these data points was excluded from further consideration.

All test results considered in the development of the recommended CGR curve are for tests performed in controlled primary water using fracture mechanics specimens, with the CGR calculated based on the average length to the crack front.* The convention of using the

* *Original footnote considered proprietary.*

"average" CGRs is consistent with ASTM practice for measuring fatigue CGRs [26,27]. In addition, average CGRs are the most appropriate rates, consistent with ASME Section XI criteria, for evaluating the time for a circumferential crack to grow until the remaining net section cannot restrain the primary pressure.

Note that the tests at Westinghouse were performed under constant load with periodic unloading, the tests at Studsvik were performed under constant load either with or without periodic unloading, the tests at EDF and CEA were performed under either constant load or constant displacement, and the tests at CIEMAT were performed under constant load using a dead load system. A review of the CGR database revealed that the potential accelerating effect of periodic unloading is relatively small, at least for susceptible materials. However, tests at constant displacement are considered likely to give artificially low values of CGR unless intergranular SCC develops over a significant proportion of the transgranular, fatigue pre-crack. For this reason, data from WOL (wedge opening load) specimens with less than 50% uniformity of crack advance across the specimen width were eliminated from further consideration.

Adjustment for effect of temperature

The rate of growth of SCC flaws in Alloy 600 is highly sensitive to temperature. As shown in Table 2, the CGR data points were adjusted to the most typical test temperature of 325°C (617°F) using an activation energy of 130 kJ/mole (31.0 kcal/mole). Based on a general consensus and input from the CGR review team, this is the recommended value for the activation energy for crack growth of Alloy 600 materials in primary water environments [1,3,28].

Form of dependence on stress intensity factor

The first step in the development of the CGR curve for Alloy 600 was to determine the form of the CGR dependence on stress intensity factor. Because of the importance of material processing parameters on the CGR, the initial evaluation was based on a heat-by-heat analysis of the database of laboratory CGRs. However, insufficient data points over a wide range of stress intensity factors were available from any single heat to determine unambiguously the form of the CGR dependence on stress intensity factor. Instead, the shape of the curve to be fitted was adopted from the Scott equation originally developed using inspection data for axial cracks in the roll transitions of steam generator tubes [2]. This CGR equation was based on hundreds of tubes and many tens of heats of very susceptible Alloy 600 material that were cracking in service at the hot leg temperature. This larger database of CGR measurements is considered to provide a more reliable indicator of the form of the dependence on stress intensity factor.

Adoption of the form of the stress intensity factor dependence of the Scott equation, developed from steam generator tubing data, results in a power-law exponent, β, of 1.16 and an apparent crack tip stress intensity factor threshold, K_{th}, of 9 MPa$\sqrt{\text{m}}$ (8.19 ksi$\sqrt{\text{in}}$). Note, however, that no actual CGR data for CRDM nozzle materials is available at K values less than approximately 15 MPa$\sqrt{\text{m}}$ (14 ksi$\sqrt{\text{in}}$), so that the implied dependence of CGR on K in this region has not been specifically verified on thick-section material. In addition, it is possible that the use of the Scott exponent results in conservative estimations of CGR at high stress intensity factors, since EDF field data [28] appear to indicate the appearance of a plateau in the CGR curve, as discussed

below (see Figure 3a). Note that other investigators in the field have also reported data that display a trend towards plateau behavior at higher stress intensity factors based on laboratory testing [29] and mechanistic modeling [30,31].

Heat-by-heat analysis

The next step in the development of the CGR curve for Alloy 600 was to consider the variability in CGR due to differences in thermomechanical material processing and material microstructure. For each of the 26 heats of material in the database, a mean power-law constant was calculated assuming the previously cited values for the activation energy, power-law exponent, and apparent stress intensity factor threshold. These 26 means were calculated based on the log values of the power-law constant α values (see Equation 2), equivalent to a least-squares fit procedure with the exponent β taken as a known constant. The function minimized by the linearized least-squares fit for each heat is $f(\alpha,\beta)$ where:

$$f(\alpha,\beta)=\sum_{i=1}^{n}\left\{\ln(\dot{a}_i)-\left[\ln(\alpha)+\beta\ln(K_i-K_{th})\right]\right\}^2 \qquad [3]$$

Table 3 shows the mean α value results for the 26 heats in both SI and English units.

Distribution of CGR variability

Insufficient data were available to derive separate CGR curves for individual heats of RVH nozzle material. Consequently, the distribution describing CGR variability was taken as the log-normal fit to the ordered median ranking of the α values for the 26 heats shown in Table 3. The resulting log-normal distribution—shown in Figure 1—is just a simple statistical fit based on the mean and standard deviation of the set of 26 log α values.* The log-mean of the log-normal distribution is -27.3358 and the log-standard deviation is 1.0160.†

MRP CGR curve for Alloy 600

Figure 2 is a standard CGR versus stress intensity factor plot showing the set of 158 points from the CGR database (Table 2) along with the CGR curve based on the 75th percentile level of the distribution of CGR variability. The MRP recommends that this curve be used to evaluate the growth of SCC flaws in thick-wall components fabricated from Alloy 600 material such as RVH nozzles including CRDM, CEDM, and In-Core Instrument (ICI) nozzles:

$$\dot{a}=\exp\left[-\frac{Q_g}{R}\left(\frac{1}{T}-\frac{1}{T_{ref}}\right)\right]\alpha(K-K_{th})^{\beta} \qquad [4]$$

where:

* The most likely estimator methodology of statistics was chosen to perform the log-normal fit since it is appropriate for this application.

† The CGR is taken in units of m/s and the stress intensity factor is taken in units of MPa $\sqrt{\text{m}}$. If the CGR is taken in units of in/yr and the stress intensity factor is taken in units of ksi $\sqrt{\text{in}}$, then the log-mean of the log-normal distribution is -6.2862 and the log-standard deviation remains 1.0160.

$\dot{a}$ = crack growth rate at temperature T in m/s (or in/yr)
Q_g = thermal activation energy for crack growth
= 130 kJ/mole (31.0 kcal/mole)
R = universal gas constant
= 8.314×10^{-3} kJ/mole·K (1.103×10^{-3} kcal/mole·°R)
T = absolute operating temperature at location of crack, K (or °R)
T_{ref} = absolute reference temperature used to normalize data
= 598.15 K (1076.67°R)
α = crack growth amplitude
= 2.67×10^{-12} at 325°C for $\dot{a}$ in units of m/s and K in units of MPa $\sqrt{\text{m}}$
(3.69×10^{-3} at 617°F for $\dot{a}$ in units of in/yr and K in units of ksi $\sqrt{\text{in}}$)
K = crack tip stress intensity factor, MPa $\sqrt{\text{m}}$ (or ksi $\sqrt{\text{in}}$)
K_{th} = crack tip stress intensity factor threshold
= 9 MPa $\sqrt{\text{m}}$ (8.19 ksi $\sqrt{\text{in}}$)
β = exponent
= 1.16

The MRP curve may be interpreted as the mean of the upper half of the distribution describing the variability in CGR due to material heat. Therefore, the MRP curve addresses the concern that heats that are more susceptible than average to crack initiation tend to have higher CGRs than average. Cracking detected in operating plants would tend to be located in components fabricated from such susceptible heats.

An important observation should be noted concerning the distribution of CGR variability developed by the MRP. Table 3 shows that the top 12 tested heats in terms of highest CGRs were all supplied by either a French supplier or B&W Tubular Products. The group of 10 tested heats supplied by Huntington, Inco, Standard Steel, Sandvik, and Sumitomo displayed lower CGRs, with log-mean power-law constants over the range from the minimum heat value to just above the distribution mean. Therefore, it is likely that components—such as RVH nozzles—supplied by some material vendors may tend to crack at a considerably lower growth rate than indicated by the full MRP database of CGR tests. There were insufficient data to confirm this conclusion, however, so a single CGR equation was adopted.

Comparison with modified Scott curve

Also shown in Figure 2 is the modified Scott curve [1,2], which was developed based on a large number of susceptible heats of steam generator tubing as previously discussed. The recommended MRP curve and modified Scott curves are in relatively close agreement, with the modified Scott curve being lower by 16%.

Comparison with available plant CGR data

There are large uncertainties in measured values of CGRs in operating plants due to the uncertainties in the measured crack growth rates, which are usually based on ultrasonic measurements of crack size at two different intervals, uncertainties in the estimates of K, which

depend on estimates of residual stress, and uncertainties in the actual operating temperatures of CRDM nozzles in different plants and in different countries. In addition, the strong heat-to-heat variation in CGRs for Alloy 600 makes it difficult to make specific comparisons for the usual case when no laboratory data are available for the heat of material involved in the field.

The most extensive measurements of CGR in operating plants are from France [28]. The French (EDF) data shown in Figure 3a have been extrapolated from the reported operating temperatures in the plants to a standard value of 325°C (617°F). In this figure, these values are compared with the results of crack growth rates predicted by using the reported *K* values for the French field data, random sampling from the upper half of the MRP distribution for CGRs, and the *K*-dependence of the Scott equation. The cumulative distributions of CGRs for the field measurements and the sample drawn from the MRP distribution are shown in Figure 3b. Because of the uncertainties in the CGRs and the lack of knowledge about the specific heats of material, good point-by-point agreement of the field and predicted data cannot be expected here. However, the predicted data show trends similar to those observed for the field data, including indications of apparent plateau-like behavior. The cumulative distributions show that the French field data are, on average, somewhat higher than the predicted values. When data showing zero crack growth are included in the field distribution, the median values differ by a factor of about 1.6. Considering the uncertainties involved, this agreement is quite reasonable and supports the choice of the 75th percentile curve from the MRP distribution as representative of the CGRs expected in CRDM nozzles that have cracked.

Repeated sampling from the MRP distribution would produce different sets of CGRs, but they will be statistically similar to those shown in Figures 3a and 3b. Occasionally, samples drawn from the tail of the log-normal distribution will give exceptionally large CGRs. This is a consequence of using a distribution which can give unrealistically high crack growth rates, albeit with low probability. In probabilistic studies, it would be more realistic to consider a distribution truncated at a suitable value, but this is not necessary for the definition of deterministic disposition curves.

The French inspection data include one example of a CRDM nozzle fabricated from *one* heat *(heat # considered proprietary)* of Alloy 600 for which laboratory measurements of CGR have also been made [28]. The plant inspection data, uncorrected for temperature, show growth rates of 0.1 to 0.5 μm/h (0.03 to 0.17 in/yr) in the depth direction and 0.3 to 1.0 μm/h (0.10 to 0.35 in/yr) for surface crack extension. These may be compared with 0.1 to 0.4 μm/h (0.03 to 0.14 in/yr) at 325°C (617°F) from laboratory tests for this heat. This is considered reasonable agreement, taking into account the various uncertainties discussed above.

For the comparison shown in Figure 3a, the EDF field data on CGR had been extrapolated from the reported head temperatures to 325°C (617°F). It is noteworthy that in no case did the actual measured CGR in the through-wall direction exceed 4 mm/yr (0.16 in/yr) for data from French plants of fundamentally Westinghouse design. This is the figure adopted in France, independent of nominal upper head temperature, to justify continued operation with axial cracks up to 11 mm (0.43 inches) deep for a one-year fuel cycle, without risk of full-thickness penetration and leakage.

A comparison of the MRP CGR curve with the limited, available plant CGR data of U.S. origin is given in Figure 2. Shown here are two data points based on the increase in length and depth of the deepest crack in D. C. Cook nozzle #75 between the initial 1994 inspection and the 1996 re-inspection [32], when the nozzle was weld repaired. These points are significantly lower than the MRP curve.

Application of the MRP Curve

The MRP recommended curve should be applied to the disposition of detected PWSCC flaws in thick-wall Alloy 600 components exposed to the primary water environment—such as axial flaws in RVH nozzle base metal material. As discussed earlier, its use at low crack-tip stress intensity factors (< approximately 15 MPa$\sqrt{m}$ (14 ksi$\sqrt{in}$)) involves assumptions not currently substantiated by actual CGR data for CRDM nozzle materials.

However, the MRP recommends that a multiplicative factor increasing the CGR be considered for evaluating the growth of hypothetical circumferential flaws connected to the OD of RVH nozzles above the elevation of the J-groove weld. Because of the current uncertainties in the exact composition of the chemical environment in contact with the nozzle OD, including the potential effect of a slightly elevated pH, the MRP recommends that a factor of 2 increase in CGR be conservatively applied for deterministic evaluations of the growth of such hypothetical, above-weld circumferential flaws. Evaluation of the growth of such circumferential flaws is required in deterministic risk assessments of potential RVH nozzle ejection and any consequential increase in core damage frequency. However, it is expected that any actual circumferential flaws detected above the J-groove weld would be repaired before plant startup.

Application of the MRP CGR curve to disposition of axial flaws in RVH nozzles

The results of an example calculation of the operating time for a detected ID axial flaw in an RVH nozzle to grow to the standard 75% through-wall acceptance limit are shown in Figure 4. The calculation assumes that the stress intensity factor is given by the expression implemented in EPRI's PWRVIA software for modeling axial PWSCC on the nozzle ID [33] and that the intact hoop stress has a magnitude of 345 MPa (50 ksi) at the location of the axial crack. Note that this example is generic in nature and should not be taken to refer to any plant-specific situation.

Application of the MRP CGR curve to deterministic evaluation of hypothetical above-weld circumferential flaws in RVH nozzles

A similar example calculation was also carried out for growth of a hypothetical circumferential crack located in an RVH nozzle above the J-groove weld. The form of the calculation is similar to the form of the calculation presented by the NRC staff in November 2001 [34,35]. First, the stress intensity factor dependence on circumferential crack size shown in Figure 5 was assumed. This dependence is from the results of finite-element facture mechanics calculations [36] currently being performed in support of MRP risk assessments. Figure 6 shows the CGR as a function of crack size calculated based on this stress intensity factor dependence and an assumed multiplicative factor of 2 on CGR to conservatively account for the current uncertainty in the composition of the OD environment.

Figures 7 and 8 show the results of integrating the CGR dependence on crack size as the crack grows around the nozzle. In particular, Figure 7 shows the operating time to grow from an initial 20° circumferential flaw to a larger size, and Figure 8 shows the operating time remaining as a function of initial crack size to grow either to the conservative failure size, or to a limit load given by 3× the design pressure (factor of safety of 3). Note that a 20° circumferential crack in a CRDM nozzle has about the same circumferential extent as the distance through the wall thickness. In addition, crack growth is assumed to occur simultaneously at both crack fronts, and the distance required for the crack to grow circumferentially was conservatively based on a horizontal—rather than oblique—section through the nozzle. Finally, for comparison purposes, the 270° and 324° crack angles assumed for the limiting sizes were taken to be the same as the values presented by the NRC staff [34,35], but these values may vary based on plant-specific parameters.

Again, the above calculation example is generic in nature and provided for illustrative purposes only.

References

1. *Crack Growth and Microstructural Characterization of Alloy 600 PWR Vessel Head Penetration Materials*, EPRI, Palo Alto, CA: 1997. TR-109136. *(Proprietary information).*

2. Scott, P. M. "An Analysis of Primary Water Stress Corrosion Cracking in PWR Steam Generators," Presented at *NEA/CSNI Specialist Meeting on Operating Experience with Steam Generators*, Brussels, Belgium, September 16–20, 1991.

3. *Minutes of Crack Growth Review Group Meeting,* Airlie House, October 2–4, 2001, EPRI, Palo Alto, CA: MRP 2002-027. *(Proprietary information).*

4. *PWR Materials Reliability Project Interim Alloy 600 Safety Assessments for US PWR Plants (MRP-44): Part 2: Reactor Vessel Top Head Penetrations*, EPRI, Palo Alto, CA: 2001. TP-1001491, Part 2. *(Proprietary information).*

5. *PWR Materials Reliability Program Response to NRC Bulletin 2001-01 (MRP-48)*, EPRI, Palo Alto, CA: 2001. 1006284. *(Proprietary information).*

6. You, D., D. Feron, and G. Turluer. "Experimental Simulation of Low Rate Primary Coolant Leaks," Presented at *Chimie 2002: Water Chemistry in Nuclear Reactors Systems: Operation Optimisation and New Developments*, French Nuclear Energy Society, Avignon, France, April 22–26, 2002.

7. *Response to NRC Review Comments Transmitted by Letter Dated June 22, 2001, to the Nuclear Energy Institute Relating to MRP-44*. Report MRP 2001-050, dated June 29, 2001, pp. 36–37. *(Proprietary information).*

8. Berge, P., D. Noel, J.-M. Gras, and B. Prieux. "Chloride Stress Corrosion Cracking of Alloy 600 in Boric Acid Solutions," *Eighth International Symposium on Environmental*

Degradation of Materials in Nuclear Power Systems—Water Reactors (Amelia Island, FL, August 10–14, 1997), Edited by S. M. Bruemmer, American Nuclear Society (ANS), La Grange Park, IL, 1997, pp. 189–199.

9. Rebak, R. B., A. R. McIlree, and Z. Szklarska-Smialowska. "Effects of pH and Stress Intensity on Crack Growth Rate in Alloy 600 in Lithiated + Borated Water at High Temperatures," *Fifth International Symposium on Environmental Degradation of Materials in Nuclear Power Systems—Water Reactors* (Monterey, CA, August 25–29, 1991), American Nuclear Society (ANS), La Grange Park, IL, 1992, pp. 511–517.

10. Rebak, R. B. and Z. Szklarska-Smialowska. "Influence of Stress Intensity and Loading Mode on Intergranular Stress Corrosion Cracking of Alloy 600 in Primary Waters of Pressurized Water Reactors," *Corrosion*, Vol. 50, No. 5, May 1994, pp. 378–393.

11. Economy, G., R. J. Jacko, and F. W. Pement. "IGSCC Behavior of Alloy 600 Steam Generator Tubing in Water or Steam Tests Above 360°C," Paper No. 250, NACE Annual Meeting, Houston, TX, March 17–21, 1986.

12. Economy, G., R. J. Jacko, and F. W. Pement. "IGSCC Behavior of Alloy 600 Steam Generator Tubing in Water or Steam Tests Above 360 C," *Corrosion–NACE*, Vol. 43, No. 12, December 1987.

13. Economy, G., R. J. Jacko, J. A. Begley, and F. W. Pement. "Influence of Hydrogen Partial Pressure on the IGSCC Behavior of Alloy 600 Tubing in 360°C Water or 400°C Steam," Paper No. 92, NACE Annual Meeting, San Francisco, CA, March 9–13, 1987.

14. Kroenke, W. C., G. Economy, R. Jacko, G. J. Powell, and B. Z. Hyatt. "Accelerated Steam Plus Hydrogen Tests for Alloy 600 Wrought and Welded Specimens," *Seventh International Symposium on Environmental Degradation of Materials in Nuclear Power Systems—Water Reactors* (Breckenridge, CO, August 7–10, 1995), NACE International, Houston, TX, 1995, Vol. 1, pp. 57–67.

15. Studsvik laboratory data provided by Anders Jenssen (Studsvik) to MRP Crack Growth Rate Review Team, October 3, 2001 (Proprietary to Studsvik). *(Proprietary information).*

16. Vaillant, F. and C. Amzallag. "Crack Growth Rates of Alloy 600 in Primary Water," Presentation to the EPRI-MRP Crack Growth Rate (CGR) Review Team, Lake Tahoe, NV, presented August 10, 2001, and revised October 11, 2001. *(Proprietary information).*

17. Vaillant, F. and S. Le Hong. *Crack Growth Rate Measurements in Primary Water of Pressure Vessel Penetrations in Alloy 600 and Weld Metal 182*, EDF, April 1997. HT-44/96/024/A. *(Proprietary information).*

18. Communications from F. Vaillant (EDF) to J. Hickling (EPRI), February 26 and April 15, 2002. *(Proprietary information).*

19. Cassagne, T., D. Caron, J. Daret, and Y. Lefèvre. "Stress Corrosion Crack Growth Rate Measurements in Alloys 600 and 182 in Primary Water Loops Under Constant Load," *Ninth International Symposium on Environmental Degradation of Materials in Nuclear Power Systems—Water Reactors* (Newport Beach, CA, August 1–5, 1999), Edited by F. P. Ford, S. M. Bruemmer, and G. S. Was, The Minerals, Metals & Materials Society (TMS), Warrendale, PA, 1999.

20. Communication from J. Hickling (EPRI) to G. White (DEI), April 29, 2002. *(Proprietary information).*

21. "Crack Growth Rate Tests of Alloy 600 in Primary PWR Conditions," Communication from M. L. Castaño (CIEMAT) to J. Hickling (EPRI), March 25, 2002. *(Proprietary information).*

22. Gómez-Briceño, D., J. Lapeña, and F. Blázquez. "Crack Growth Rates in Vessel Head Penetration Materials," *Proceedings of the International Symposium Fontevraud III: Contribution of Materials Investigation to the Resolution of Problems Encountered in Pressurized Water Reactors* (Chinon, France, September 12–16, 1994), French Nuclear Energy Society, Paris, 1994, pp. 209–214.

23. Gómez-Briceño, D. and J. Lapeña. "Crack Growth Rates in Vessel Head Penetration Materials," *Proceedings: 1994 EPRI Workshop on PWSCC of Alloy 600 in PWRs* (Tampa, FL, November 15–17, 1994), EPRI, Palo Alto, CA, TR-105406, August 1995, pp. E4-1 through E4-15. *(Proprietary information).*

24. Gómez-Briceño, D., et al. "Crack Propagation in Inconel 600 Vessel Head Penetrations," Eurocorr 96, Nice, France, September 24–26, 1996.

25. Castaño, M. L., D. Gómez-Briceño, M. Alvarez-de-Lara, F. Blázquez, M. S. Garcia, F. Hernández, and A. Lagares. "Effect of Cationic Resin Intrusions on IGA/SCC of Alloy 600 Under Primary Water Conditions," *Proceedings of the International Symposium Fontevraud IV: Contribution of Materials Investigation to the Resolution of Problems Encountered in Pressurized Water Reactors* (France, September 14–18, 1998), French Nuclear Energy Society, Paris, 1998, Volume 2, pp. 925–937.

26. "Standard Test Method for Measurement of Fatigue Crack Growth Rates," American Society for Testing and Materials, West Conshohocken, PA, 1995. ASTM Standard E647–95a.

27. "Standard Test Method for Plane-Strain Fracture Toughness of Metallic Materials," American Society for Testing and Materials, West Conshohocken, PA, 1990. ASTM Standard E399–90.

28. Amzallag, C. and F. Vaillant. "Stress Corrosion Crack Propagation Rates in Reactor Vessel Head Penetrations in Alloy 600," *Ninth International Symposium on Environmental Degradation of Materials in Nuclear Power Systems—Water Reactors* (Newport Beach, CA, August 1–5, 1999), Edited by F. P. Ford, S. M. Bruemmer, and G. S. Was, The Minerals, Metals & Materials Society (TMS), Warrendale, PA, 1999, pp. 235–241.

29. Magdowski, R. and M. O. Speidel. "Major Influences on the Growth Rates of Stress Corrosion Cracks in Alloy 600 Exposed to Simulated Primary Water," *Proceedings: 1997 EPRI Workshop on PWSCC of Alloy 600 in PWRs* (Daytona Beach, FL, February 25–27, 1997), EPRI, Palo Alto, CA, TR-109138-P2, November 1997, pp. E11-1 through E11-16. *(Proprietary information).*

30. Hall, Jr., M. M. "Environment-Assisted Creep Fracture Model for Primary Water Stress Corrosion Cracking of Alloy 600," *Proceedings: 1997 EPRI Workshop on PWSCC of Alloy 600 in PWRs* (Daytona Beach, FL, February 25–27, 1997), EPRI, Palo Alto, CA, TR-109138-P2, November 1997, pp. E12-1 through E12-34. *(Proprietary information).*

31. Hall, Jr., M. M. and D. M. Symons. "Hydrogen Embrittlement Mechanism for Low Potential Stress Corrosion Cracking of Nickel Base Alloys: Hydrogen-Assisted Creep Fracture Model," *Proceedings: 2000 EPRI Workshop on PWSCC of Alloy 600 in PWRs (PWRMRP-27)* (St. Pete Beach, FL, February 14–16, 2000), EPRI, Palo Alto, CA, 1000873, November 2000, pp. D12-1 through D12-46. *(Proprietary information).*

32. Bamford, W. H. "D. C. Cook Unit 2 Upper Head Penetration Crack Growth Determined from Inspection Data," Westinghouse Electric Company, LLC, November 2001. LTR-SMT-01-72. *(Proprietary information).*

33. *CHECWORKS™ PWR Vessel and Internals Application: RPV Head Nozzle Module, Version 1.1, User Guide*, EPRI, Palo Alto, CA: 1999. TR-103198-P8. *(Proprietary information).*

34. U.S. Nuclear Regulatory Commission. *Preliminary Staff Technical Assessment for Pressurized Water Reactor Vessel Head Penetration Nozzles Associated with NRC Bulletin 2001-01, "Circumferential Cracking of Reactor Pressure Vessel Head Penetration Nozzles,"* November 2001, proprietary designation removed December 4, 2001.

35. U.S. Nuclear Regulatory Commission (A. Hiser). "Deterministic and Probabilistic Assessments," Presentation at Meeting Between the NRC Staff and the Materials Reliability Program to Discuss NRC Bulletin 2001-01, Rockville, MD, November 8, 2001.

36. Preliminary Results of Stress Intensity Factor Calculations for Circumferential Crack Growth in CRDM Nozzles, Structural Integrity Associates, E-mail from P. Riccardella (SIA) to G. White (DEI), January 31, 2002. *(Proprietary information).*

Table 1.
Key Technical Issues in Assessing Alloy 600 Laboratory Crack Growth Rate Tests

1	Material within specifications including condition/heat treatment
2	Composition within material specifications
3	Mechanical strength properties
4	ASTM specimen size criteria
5	Straightness criteria and crack front mapping
6	Standard procedure for welds
7	Environment (Li, B, and H_2 concentrations; hydrogen control; temperature; ECP)
8	Loop configuration (e.g., once-through, refreshed, static with H_2 control) and flow rate
9	Water chemistry confirmation (e.g., Cl, SO_4)
10	Crack length confirmed by destructive examination
11	Transgranular fraction on fractograph
12	Fraction SCC along crack front
13	Changing conditions during a test?
14	Active constant or cyclic loading versus constant displacement loading (e.g., wedge loading)
15	Load during “cool down”
16	Crack length versus time data
17	SCC crack increment
18	Precision on measurement of crack length increase

Table 2.
Laboratory Alloy 600 CGR Data Used to Develop the MRP CGR Distribution

(Laboratory Alloy 600 CGR Data Used to Develop the MRP CGR Distribution removed as proprietary)

Table 2 (continued).
Laboratory Alloy 600 CGR Data Used to Develop the MRP CGR Distribution

Table 3.
Mean CGR Power-Law Constant α for Each Alloy 600 Heat in Laboratory Database

(The material heat identifiers are considered proprietary information and have been removed from the second column of the following table.)

Heat Rank		Material Supplier	Product Form	Number of Data Points	Log Mean Power-Law Constant α at 325°C (617°F)	
					SI Units[1]	English Units[2]
1		Creusot-Imphy	Forged Bar	21	6.01E-12	8.32E-03
2		B&WTP	Thick-wall Tube	4	5.16E-12	7.15E-03
3		French Supplier	CRDM Nozzle	9	5.08E-12	7.03E-03
4		Tecphy	Rolled Bar	7	4.96E-12	6.88E-03
5		B&WTP	Thick-wall Tube	4	4.71E-12	6.52E-03
6		VDM	Rolled Plate	2	3.92E-12	5.43E-03
7		Schneider-Creusot	Forged Bar	1	3.19E-12	4.42E-03
8		B&WTP	Thick-wall Tube	32	3.07E-12	4.25E-03
9		B&WTP	Thick-wall Tube	1	2.65E-12	3.68E-03
10		Arbed	CRDM Nozzle	3	2.01E-12	2.79E-03
11		Creusot-Imphy	Forged Plate	1	1.94E-12	2.69E-03
12		Schneider-Creusot	Forged Bar	1	1.62E-12	2.24E-03
13		Huntington	Thick-wall Tube	1	1.37E-12	1.90E-03
14		Huntington	Rolled Plate	14	1.29E-12	1.78E-03
15		*Not Listed*	Forged Bar	2	1.02E-12	1.41E-03
16		Sumitomo Metal	Thick-wall Tube	1	1.01E-12	1.40E-03
17		Sandvik	Thick-wall Tube	27	1.00E-12	1.39E-03
18		Standard Steel	Forged Bar	1	9.09E-13	1.26E-03
19		Huntington	Thick-wall Tube	12	7.21E-13	9.99E-04
20		*Not Listed*	Forged Bar	3	6.31E-13	8.74E-04
21		Tecphy	Rolled Bar	1	5.18E-13	7.18E-04
22		Huntington	Plate	1	4.97E-13	6.89E-04
23		Creusot-Ondaine	Forged Bar	4	4.44E-13	6.15E-04
24		Inco	Rolled Bar	1	2.51E-13	3.48E-04
25		Sandvik	Thick-wall Tube	2	2.18E-13	3.03E-04
26		Huntington	Thick-wall Tube	2	1.93E-13	2.67E-04
		Log-Mean for All Data Points		158	1.96E-12	2.72E-03
		Log-Mean of Heat Log-Means		26 Heats	1.34E-12	1.86E-03

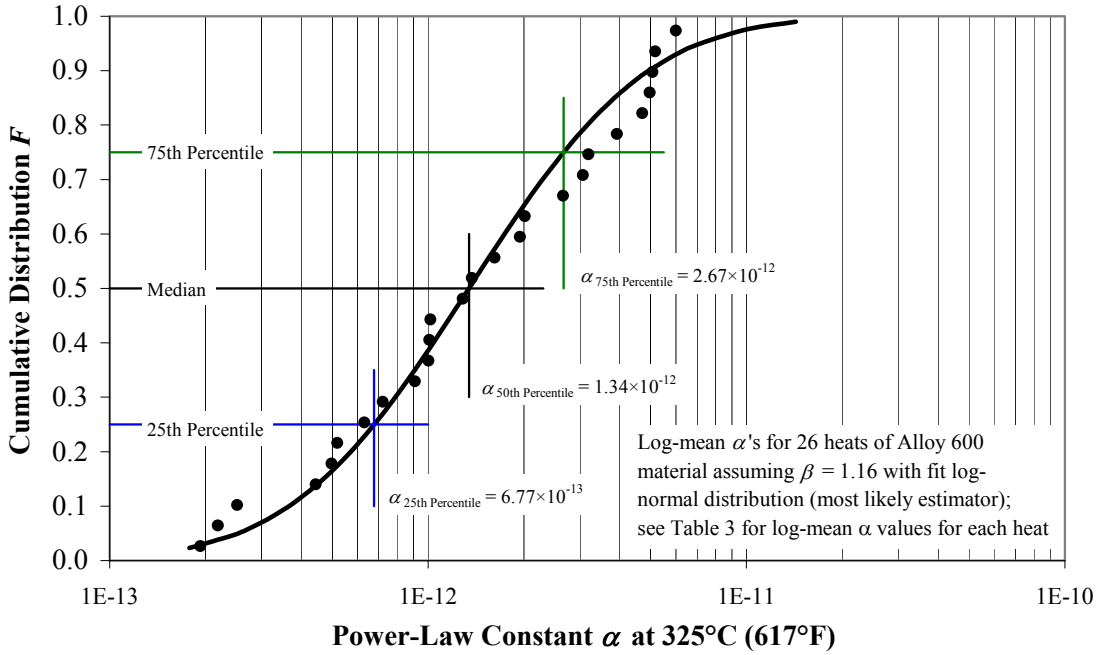

Figure 1. Log-Normal Distribution Fit of Log Mean Power-Law Constants for 26 Alloy 600 Heats Assuming Exponent of 1.16

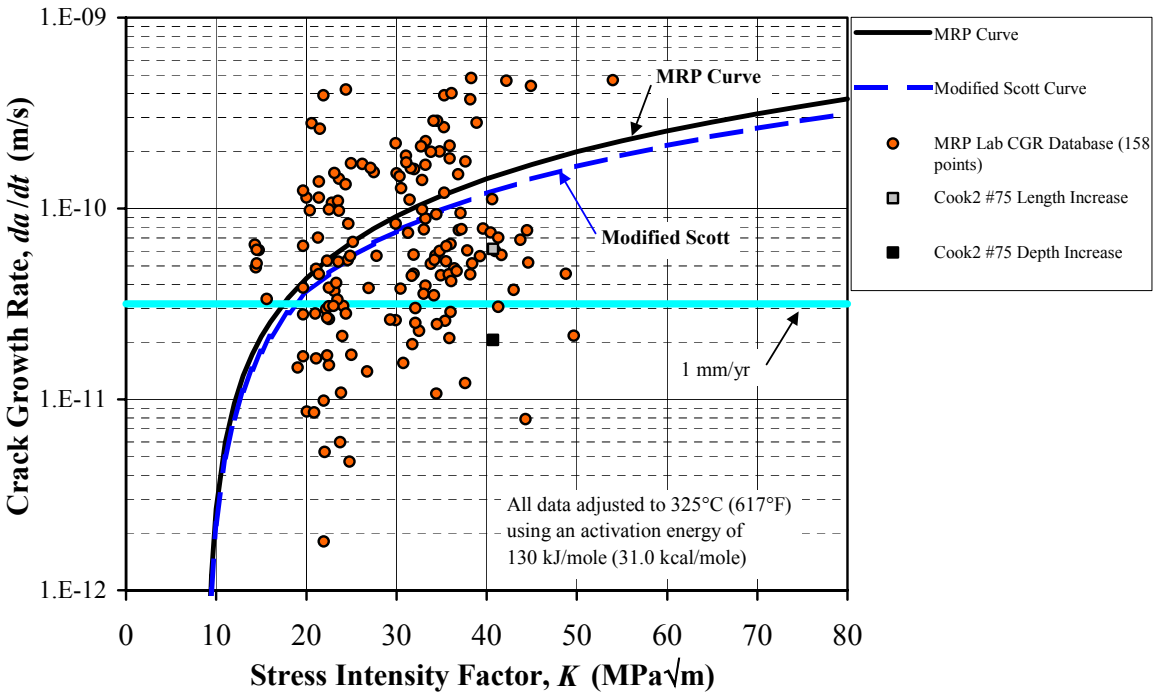

Figure 2. Screened Laboratory Data for Alloy 600 with the MRP Crack Growth Curve, the Modified Scott Curve [1], and CGR Data for Cook 2 Nozzle #75 [32]

(non-proprietary version of figure)

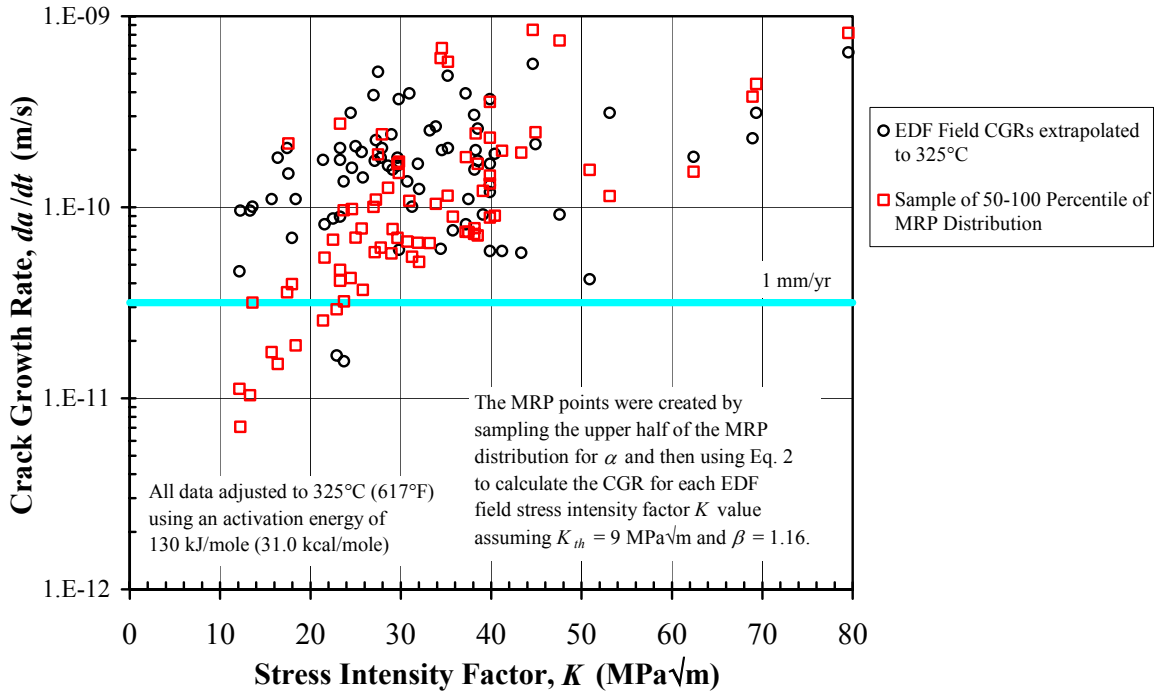

Figure 3a. Comparison of EDF Field Data for CRDM Nozzles* [28] with Predictions of CGRs Obtained by Sampling the Upper Half of the MRP Distribution

* Extrapolated to a common temperature of 325°C.

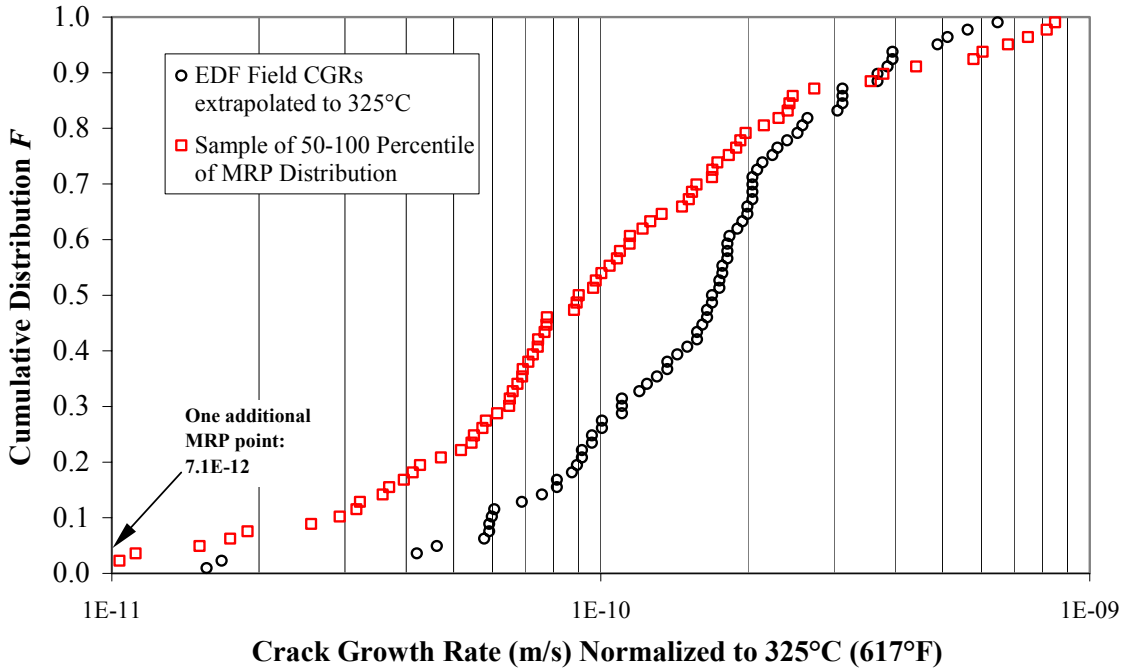

Figure 3b. Cumulative Distribution of Temperature-Adjusted EDF Field CGRs and Those Drawn from the 50th to 100th Percentile of the MRP CGR Distribution

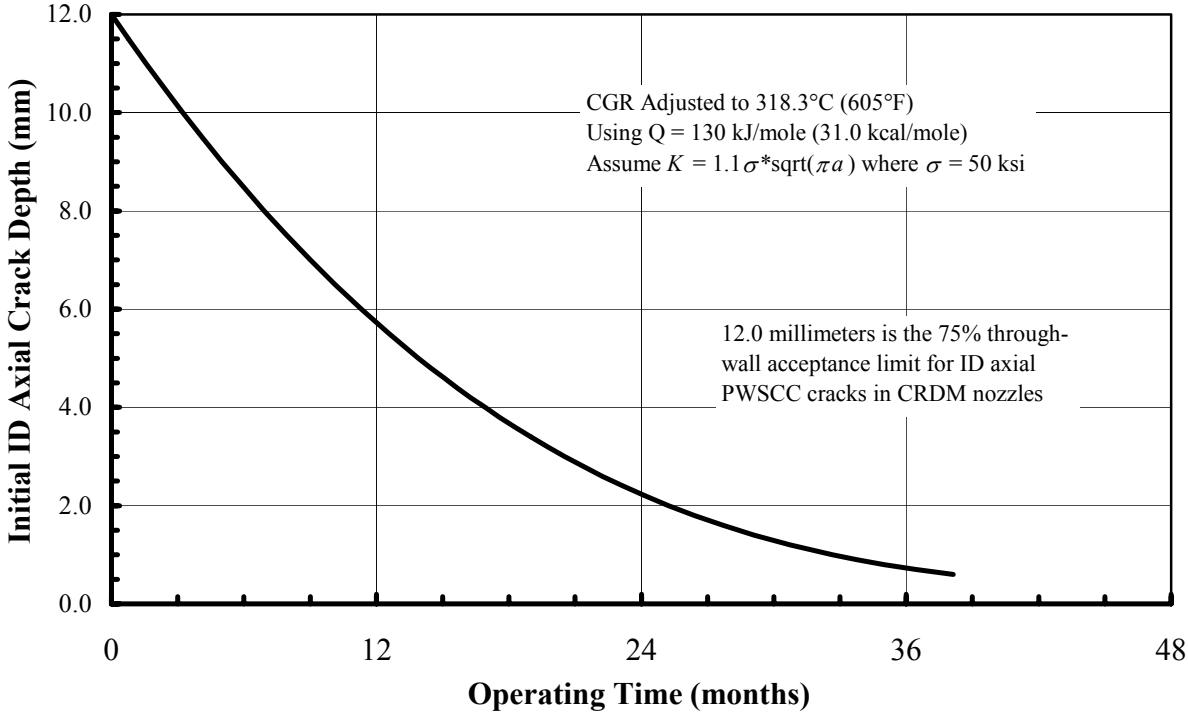

Figure 4. Example Calculation of Remaining Operating Time for an ID Axial Crack to Grow to a Depth of 12 Millimeters at the Maximum U.S. Head Temp. of 605°F

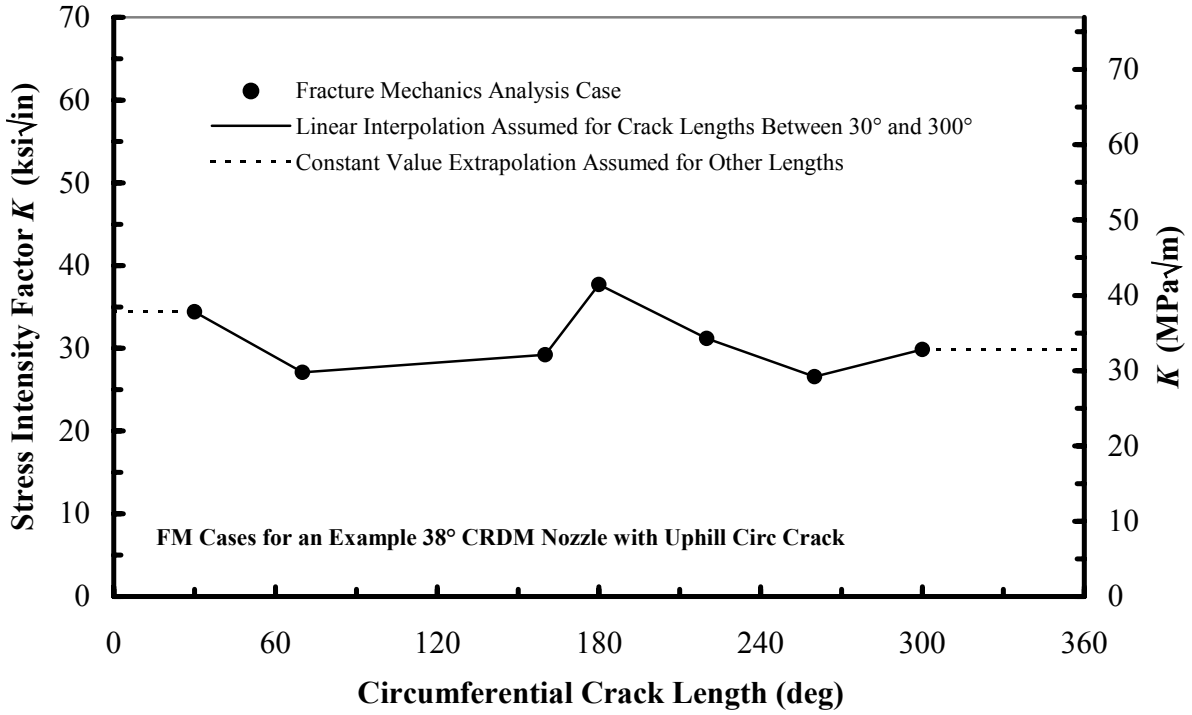

Figure 5. Crack Tip Stress Intensity Factor Calculated by SIA [36] Assumed to Produce the Circumferential Crack Growth Results Shown in Figures 6 to 8

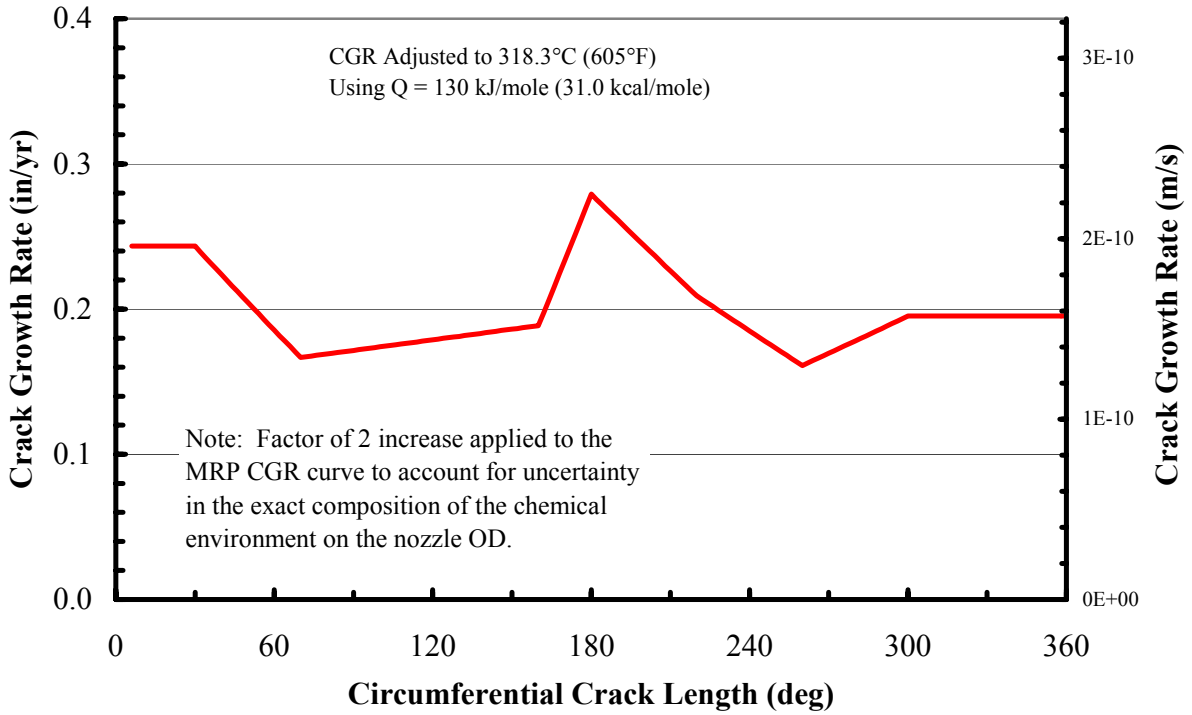

Figure 6. Calculated Rate of Circumferential Crack Growth at the Maximum U.S. Head Temperature of 605°F

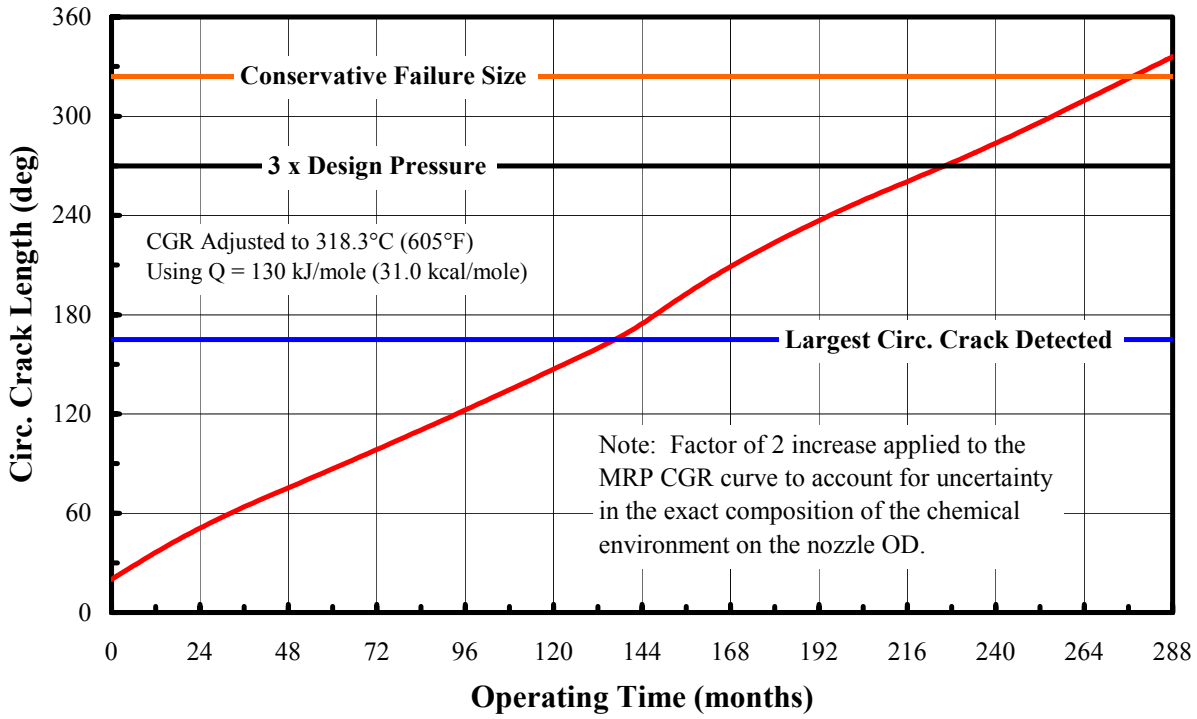

Figure 7. Calculated Operating Time for an Initial 20° Circumferential Crack to Grow to a Larger Size at the Maximum U.S. Head Temperature of 605°F

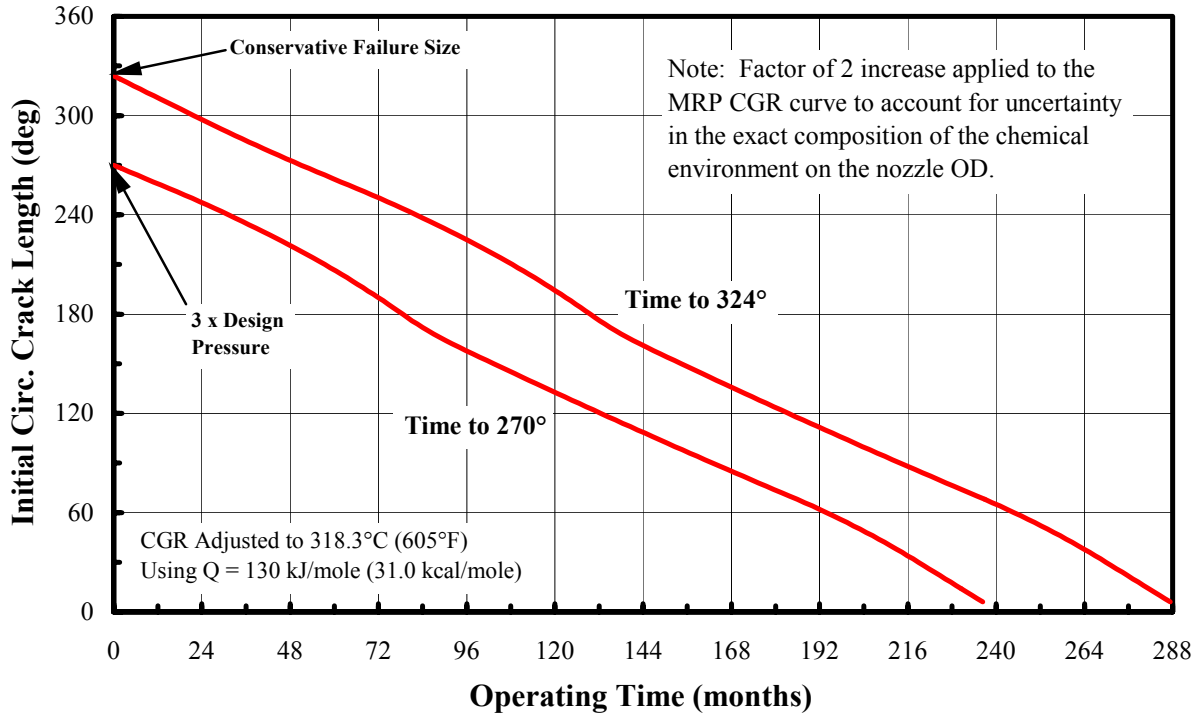

Figure 8. Calculated Remaining Operating Time for a Circumferential Crack to Grow to the 3× Limit Load Condition or the Failure Size at a Head Temp. of 605°F

Appendix A.
Laboratory Alloy 600 CGR Data Excluded in the Development of MRP CGR Distribution

(removed as proprietary)